JVI Journals.ASM.org

Herpes Simplex Virus 1 Serine/Threonine Kinase US3 Hyperphosphorylates IRF3 and Inhibits Beta Interferon Production

Shuai Wang,[a,b] Kezhen Wang,[a,b] Rongtuan Lin,[c] Chunfu Zheng[a,b]

Soochow University, Institutes of Biology and Medical Sciences, Suzhou, China[a]; Molecular Virology and Viral Immunology Research Group, Wuhan Institute of Virology, Chinese Academy of Sciences, Wuhan, China[b]; Lady Davis Institute for Medical Research, Department of Medicine, McGill University, Montreal, Quebec, Canada[c]

Viral infection initiates a series of signaling cascades that lead to the transcription of interferons (IFNs), finally inducing interferon-stimulated genes (ISGs) to eliminate viruses. Viruses have evolved a variety of strategies to modulate host IFN-mediated immune responses. Herpes simplex virus 1 (HSV-1) US3, a Ser/Thr kinase conserved in alphaherpesviruses, was previously reported to counteract host innate immunity; however, the molecular mechanism is elusive. In this study, we report that US3 blocks IFN-β production by hyperphosphorylating IFN regulatory factor 3 (IRF3). Ectopic expression of US3 protein significantly inhibited Sendai virus (SeV)-mediated activation of IFN-β and IFN-stimulated response element (ISRE) promoters and the transcription of IFN-β, ISG54, and ISG56. US3 was also shown to block SeV-induced dimerization and nuclear translocation of IRF3. The kinase activity was indispensable for its inhibitory function, as kinase-dead (KD) US3 mutants K220M and D305A could not inhibit IFN-β production. Furthermore, US3 interacted with and hyperphosphorylated IRF3 at Ser175 to prevent IRF3 activation. Finally, the US3 KD mutant viruses were constructed and denoted K220M or D305A HSV-1, respectively. Cells and mice infected with both mutant viruses produced remarkably larger amounts of IFN-β than those infected with wild-type HSV-1. For the first time, these findings provide convincing evidence that US3 hyperphosphorylates IRF3, blocks the production of IFN-β, and subverts host innate immunity.

Innate immunity is a conserved, rapid defense mechanism against pathogen invasion. The type I interferon (IFN-I) pathway plays a crucial role in mediating the antiviral response through induction of a diverse set of IFN-stimulated genes (ISGs) (1). Following viral infection, the pattern recognition receptors of the host cell, including the Toll-like receptor (TLR) and retinoic acid-inducible gene I (RIG-I)-like receptor (RLR) families, recognize viral-pathogen-associated molecular patterns, which are usually viral nucleic acids (single-stranded RNA [ssRNA], double-stranded RNA [dsRNA], and single-stranded DNA [ssDNA]), leading to the activation of transcription factors NF-κB and IFN regulatory factors 3 and 7 (IRF3/7). The activation and nuclear translocation of these transcription factors subsequently induce the production of type I IFNs, namely, IFN-α and IFN-β, which induce the expression of ISGs and inhibit the replication of virus (2–4).

Herpes simplex virus 1 (HSV-1) is the archetypal member of the alphaherpesvirus subfamily, with a large, linear dsDNA virus genome of 152 kb. HSV-1 encodes a viral Ser/Thr kinase, US3, which is conserved in the alphaherpesvirus subfamily but is not present in other herpesviral genomes. Increasing evidence indicates that US3 protein kinase is involved in multiple processes during viral infection, including nuclear egress, virion maturation (5–8), prevention of apoptosis (9–15), rearrangements of the cytoskeleton, promotion of cell-to-cell spread during viral infection (16–18), blocking of histone deacetylation by phosphorylation of histone deacetylase 1 and 2 (HDAC1/2) (19–21), disruption of promyelocytic leukemia protein nuclear bodies (PML-NBs) (22), and downregulation of major histocompatibility complex class I (MHC-I) surface expression (23). US3 is also reported to masquerade as the cellular kinase Akt to phosphorylate tuberous sclerosis complex 2 (TSC2), leading to constitutive activation of mammalian target of rapamycin complex 1 (mTORC1) and inhibition of the translational repressor 4E-binding protein 1 (4E-BP1) and enhancing viral gene expression (24, 25).

To complete their life cycles, viruses have evolved strategies to evade the innate antiviral responses. HSV-1 evolves multiple immune evasion strategies to inhibit the IFN-signaling pathway. For example, HSV-1 infected cellular protein 0 (ICP0) blocks IFN production by targeting IRF3 (26–29) and HSV-1 ICP34.5 inhibits IFN production by binding and sequestering TANK-binding kinase 1 (TBK1) (30, 31). The HSV-2 virion host shutoff protein (Vhs) was reported to suppress IFN and ISG induction by degrading cellular mRNA (32, 33). ICP27 was also suggested to inhibit IFN responses. Viruses lacking ICP27 induce higher levels of cytokines, including IFN, in monocytic cells than the wild-type (WT) virus (34, 35). HSV-1 Us11 inhibited IFN-β production via directly binding to RIG-I and melanoma differentiation-associated antigen 5 (MDA-5) (36). Our group identified HSV-1 VP16 as a novel antagonist of IFN-β by inhibiting NF-κB activation and blocking IRF3 to recruit its coactivator, CREB-binding protein (CBP) (37). Recently, HSV-1 UL36 ubiquitin-specific protease (UL36USP) was proven to counteract IFN-β production by deubiquitinating tumor necrosis factor receptor-associated factor 3 (TRAF3) (38).

HSV-1 US3 is suggested to play an important role in immune evasion during HSV-1 infection. Piroozmand et al. found that when there was a low multiplicity of infection (MOI), US3-null HSV-1 was more sensitive to IFN-α than the WT virus, suggesting

Received 19 August 2013 **Accepted** 14 September 2013
Published ahead of print 18 September 2013
Address correspondence to Chunfu Zheng, zheng.alan@hotmail.com.

doi:10.1128/JVI.02355-13

that US3 afforded resistance to IFN-α treatment (39). Liang et al. demonstrated that US3 blocks IFN-γ-induced ISG expression by phosphorylating the alpha subunit of the IFN-γ receptor (40). Peri et al. reported that HSV-1 US3 counteracts the TLR3-mediated response by reducing the expression of TLR3 and that US3-null HSV-1 resulted in strong activation of IRF3 and the type I IFN response (41). Recently, US3 protein kinase was proven to be necessary and sufficient to suppress extracellular-signal-regulated kinase activity and subvert host mitogen-activated protein kinase-signaling pathways (42).

Although increasing evidence has shown that HSV-1 US3 antagonizes the host innate immune system, the mechanism by which US3 interrupts innate immunity, especially the RLR-mediated IFN-β production pathway, needs to be further characterized. In this study, we investigated the molecular mechanism by which US3 blocks IFN-β production. We found that ectopic expression of US3 significantly downregulated Sendai virus (SeV)-activated IFN-β promoter activity and that the protein kinase activity of US3 was indispensable for the inhibitory activity. Additionally, US3 interacted with and hyperphosphorylated IRF3 to induce atypical phosphorylation of IRF3. Finally, infection with US3 kinase-dead (KD) mutant HSV-1 resulted in increased production of IFN-β. To our knowledge, this is the first report identifying IRF3 as a US3 substrate, and thus these findings reveal a novel mechanism for HSV-1 to evade host antiviral immunity.

MATERIALS AND METHODS

Cells, viruses, and antibodies. HEK 293T cells and Vero cells were grown in Dulbecco's modified Eagle medium (DMEM) (Gibco-BRL) supplemented with 10% fetal bovine serum (FBS) and 100 U/ml of penicillin and streptomycin. HeLa cells were maintained in Eagle's minimum essential medium (MEM) (Gibco-BRL) supplemented with 10% FBS.

The WT HSV-1 F strain and its derivative, US3 mutant HSV-1, were propagated in Vero cells and titrated as described previously (43). Sendai virus (SeV) was propagated and titrated as described previously (36).

Protease inhibitor cocktails were purchased from Cell Signaling Technology, Inc. (Boston, MA). Mouse anti-Myc, anti-Flag, and anti-hemagglutinin (HA) monoclonal antibodies (MAbs) were purchased from ABmart (Shanghai, China). Mouse monoclonal IgG1 and IgG2b isotype control antibodies were purchased from eBioscience, Inc. (San Diego, CA). Rabbit anti-IRF3 polyclonal antibody (pAb) and mouse anti-β-actin MAb were purchased from Santa Cruz Biotechnology (Santa Cruz, CA). Rabbit antibody against IRF3-S396 was previously described (44). Rabbit antibodies against HSV-1 UL42, UL46, and US3 were made by GL Biochem Ltd. (Shanghai, China).

Plasmid construction. All enzymes except for T4 DNA ligase (New England BioLabs, Massachusetts) that were used for cloning procedures were purchased from TaKaRa (Dalian, China). To construct US3-Flag, we amplified the open reading frame (ORF) of US3 from plasmid US3-EYFP as previously described (45) and cloned it into the BglII and EcoRI sites of the pCMV-Flag vector (Beyotime, Shanghai, China). Commercial reporter plasmids used include NF-κB-Luc (Stratagene, La Jolla, CA) and pRL-TK (Promega). Gift plasmids used include the following: (pRDIII-I)4-Luc (46), pcDNA3.1-FlagTBK1 and pcDNA3.1/Zeo-MAVS (47), pcDNA3.1-FlagIKKε (48), pEF-Flag-RIG-IN (49), IRF3/5D (50), pCAGGS-NS1 (51), and IFN-β promoter reporter plasmid (52).

RNA isolation and quantitative PCR. Total RNA was extracted from HEK 293T cells with TRIzol (Invitrogen, California) according to the manufacturer's manual. Samples were digested with DNase I and subjected to reverse transcription as previously described (53). The cDNA was used as a template for quantitative PCR to investigate the expression patterns of human IFN-β, ISG54, and ISG56. Detailed protocols have been previously described (54).

Transfection and dual-luciferase reporter (DLR) assays. HEK 293T cells were plated on 24-well dishes (Corning, NY) in DMEM (Gibco-BRL, Maryland) with 10% FBS at a density of 1×10^5 cells per well overnight before transfection as previously described (44). Cells were then cotransfected with 1 μg of expression plasmid, 500 ng of a reporter plasmid such as IFN-β-Luc, NF-κB-Luc, or (pRDIII-I)4-Luc, and 50 ng of pRL-TK *Renilla* luciferase reporter plasmid to normalize transfection efficiency, as indicated by standard calcium phosphate precipitation (55, 56). At 24 h posttransfection, cells were infected with SeV (100 hemagglutination units [HAU]/ml) for 16 h, and luciferase assays were performed as previously described (44) with a luciferase assay kit (Promega, Madison, WI). Poly(I·C) and poly(dA-dT) were purchased from InvivoGen.

Immunofluorescence assays. Immunofluorescence assays were performed as described previously (57). In brief, HeLa cells were tansfected with the US3-Flag, K220M-Flag, or D305A-Flag plasmid for 12 h and then fixed in 4% paraformaldehyde. Cells were incubated with rabbit anti-IRF3 pAb (diluted 1:500) or with mouse anti-Flag MAb (diluted 1:2,000), followed by incubation with tetramethyl rhodamine isocyanate (TRITC)-conjugated goat anti-rabbit IgG (Pierce) and fluorescein isothiocyanate (FITC)-conjugated goat anti-mouse IgG (Sigma-Aldrich). After each incubation step, cells were washed extensively with phosphate-buffered saline (PBS). Samples were analyzed with fluorescence microscopy (Zeiss, Germany).

Western blot analysis. Western blot (WB) analysis was performed as previously described (43). Briefly, whole-cell extracts were subjected to 10% SDS-PAGE and transferred to polyvinylidene difluoride (PVDF) or nitrocellulose membranes followed by blocking with 5% nonfat milk in Tris-buffered saline–Tween (TBST) and probed with anti-Flag, HA, Myc, IRF3, IRF3-S396, HSV-1 ICP0, UL42, UL46, US3, or β-actin antibody according to product manuals. After being washed with TBST, the membranes were incubated with alkaline phosphatase (AP)-conjugated goat anti-rabbit IgG or goat anti-mouse IgG. Protein bands specific to the antibody were developed by 5-bromo-4-chloro-3-indolylphosphate (BCIP)–nitroblue tetrazolium (NBT); development was terminated with distilled water.

Coimmunoprecipitation assays. Coimmunoprecipitation (co-IP) assays were performed as previously described (43). Briefly, HEK 293T cells ($\sim 5 \times 10^6$) were cotransfected with 10 μg of Flag-US3 expression plasmid. Transfected cells were harvested at 24 h posttransfection and lysed on ice with 500 μl of lysis buffer. The lysates were incubated with 0.5 μg of the Flag antibodies and 30 μl of a 1:1 slurry of protein A/G plus agarose beads (Santa Cruz, California) overnight at 4°C. The beads were washed four times with 1 ml of lysis buffer containing 500 mM NaCl, and WB analysis was performed to detect endogenous IRF3 using IRF3 antibody. The co-IP assays were repeated twice.

Native PAGE. Native PAGE was carried out using Ready Gels (7.5%; Bio-Rad). Gels were prerun with 25 mM Tris and 192 mM glycine [pH 8.4] with 1% deoxycholate (DOC) in a cathode chamber for 30 min at 40 mA. Samples in native sample buffer (10 μg protein, 62.5 mM Tris-Cl [pH 6.8], 15% glycerol, and 1% DOC) were size fractionated by electrophoresis for 60 min at 25 mA and transferred to nitrocellulose membranes for WB analysis as previously described (58).

Purification of US3-GST and IRF3-His and *in vitro* protein kinase assay. The ORF of IRF3 was cloned into pET15b and transformed into *Escherichia coli* Rossetta cells. After treatment with 0.1 mM isopropyl-β-D-thiogalactopyranoside (IPTG) for 3 h, the recombinant protein US3-His was purified with His-Bind resin (Novagen) according to the manufacturer's manual.

Purification of US3-GST, K220M-GST, and D305A-GST fusion proteins and kinase assays were performed according to previously described methods with minor modifications (59). Plasmid expressing US3, K220M, or D305A fused to glutathione *S*-transferase (GST) was transfected into HEK 293T cells. After 24 h, the cell lysates were incubated with 200 μl of a 50% slurry of glutathione-Sepharose beads (Novagen) overnight. The beads were extensively washed with PBS, and recombinant

proteins were eluted with GST elution buffer (5 mM glutathione, 50 mM Tris-HCl [pH 8.0]).

Two micrograms of purified US3-GST, K220M-GST, or D305A-GST and 0.2 μg of IRF3-His were incubated in US3 kinase buffer (50 mM Tris-HCl [pH 9.0], 20 mM $MgCl_2$, 0.1% NP-40, 1 mM dithiothreitol [DTT], and 10 μM ATP) at 37°C overnight, and WB assays were performed to detect the phosphorylated IRF3.

Recombinant virus construction. Construction of the K220M, D305A, and repaired-HSV-1 mutants was based on a luciferase-tagged infectious HSV-1 bacterial artificial chromosome (BAC) described in our previous papers (60, 61). Amplification of the Kan^r cassette was done by PCR with a pair of primers containing a 40-bp-homology flanking sequence of US3. PCR product was then transformed into *E. coli* DY380-competent cells carrying the pHSV-1 BAC via electroporation, and the US3 gene was replaced with the Kan^r cassette by homologous recombination to create the pHSV-1 BAC ΔUS3 clone. Then a US3 fragment containing the K220M, D305A, or US3 mutant was cloned into the plasmid pGEM-Lox-Zeo to construct pK220M-Zeo, pD305A-Zeo, or pUS3-Zeo. PCR was performed to amplify the K220M-Zeo^r, D305A-Zeo^r, and US3-Zeo^r cassettes with a pair of primers containing a 40-bp-homology flanking sequence of US3. Then the PCR products were transformed into *E. coli* DY380 cells containing the pHSV-1 BAC ΔUS3 clone. The Kan^r cassette was replaced with the K220M-Zeo^r or D305A-Zeo^r cassette by homologous recombination to create the pHSV-1 BAC K220M-Zeo^r and D305A-Zeo^r clones. To reconstitute recombinant viruses, Vero cells were transfected with 2 μg of the corresponding BAC DNA via electroporation. To remove the Zeo^r gene (flanked by two *loxP* sites) from the HSV-1 genome, we cotransfected a Cre expression plasmid (pGS403) (see Fig. 7A).

Two-step red-mediated recombination was applied to construct US3-Flag mutant HSV-1 (62). A Kan^r cassette was amplified by PCR with a pair of primers containing a 40-bp-homology flanking sequence of mutant sites and a Flag tag sequence. Then PCR product was transformed into *E. coli* GS1783-competent cells carrying the pHSV-1 BAC via electroporation. PCR assays were used to identify positive clones. L-Arabinose was used to induce a second red recombination to delete the Kan^r cassette (see Fig. 5B).

To analyze the integrity of the BAC clones, we digested 15 μg of BAC DNA with EcoR I or BamH I and compared the restriction pattern of BAC DNA to that of WT BAC (data not shown). The recombinant viruses were validated by PCR and sequencing using primers upstream or downstream of US3 (data not shown). Viruses were harvested and the growth kinetics of the recombinant viruses were characterized by both traditional plaque assay and luciferase activity assay in Vero cells at an MOI of 0.1 or 1. A luciferase activity assay was performed with a luciferase assay kit (Promega, Madison, WI).

ELISA for IFN-β. An enzyme-linked immunosorbent assay (ELISA) to quantify secreted IFN-β was carried out with culture supernatants collected from infected cells as previously described (36). Briefly, cell culture medium was collected and centrifuged to remove cell debris. A human IFN-β ELISA kit (PBL Interferon Source, Piscataway NJ) was used to detect the IFN-β according to the manufacturer's instructions.

Four-week-old female C57BL/6 mice were purchased from the Experimental Animal Center, Wuhan Institute of Virology, Chinese Academy of Sciences. The mice were injected intraperitoneally with 10^6 PFU of the WT, K220M, or D305A, or repaired HSV-1. After 24 h, mice were sacrificed and a Legend Max mouse IFN-β ELISA kit (BioLegend, San Diego, CA, USA) was applied to detect the IFN-β in serum. The animal study proposal was approved by the Institutional Animal Care and Use Committee (IACUC) of the Experimental Animal Center, Wuhan Institute of Virology, Chinese Academy of Sciences. The approved protocol number is IACUC2012059. All mouse experimental procedures were done according to the Regulations for the Administration of Affairs Concerning Experimental Animals approved by the State Council of the People's Republic of China.

RESULTS

US3 inhibits the SeV-mediated activation of the IFN-β and ISRE promoters. To examine the function of US3 in the regulation of virus-mediated activation of the IFN-β promoter, we coexpressed US3 in HEK 293 cells in the presence of IFN-β reporter genes. SeV infection resulted in an ~450-fold induction of IFN-β-Luc reporter activity. Transfection of 50 ng and 500 ng of US3 expression plasmids inhibited SeV-mediated activation of IFN-β promoter activity by 90.1% and 95.3%, respectively (Fig. 1A). US3 was also demonstrated to significantly inhibit SeV-induced activation of the IFN-stimulated response element (ISRE) using an ISRE reporter plasmid. Fifty nanograms and 500 ng of US3 expression plasmids exhibited 54% and 89% inhibitory activity, respectively (Fig. 1B). Transcription of the IFN-β gene required IRF3 and other transcription factors to bind to distinct regulatory domains in the IFN-β promoter. To investigate whether US3 inhibited the SeV-induced activation of IRF3, we performed reporter gene assays with HEK 293 cells using the luciferase reporter plasmid driven by tandem IRF binding site positive regulatory domains I and III [PRD(III-I)] regulatory elements from the IFN-β promoter [(pRD(III-I)4-Luc]. The result showed that SeV infection induced strong IRF-responsive PRD(III-I) promoter activity, and transfection of 50 ng and 500 ng of US3 expression plasmids remarkably inhibited SeV-induced PRD(III-I) reporter activities by 86% and 92%, respectively (Fig. 1C). Furthermore, US3-inhibited SeV-induced expression of IFN-β was detected by real-time PCR. SeV infection induced about a 50-fold increase in IFN-β mRNA expression, which was significantly inhibited by ectopic expression of US3 (Fig. 1D). Poly(I·C) and poly(dA-dT) are known as synthetic analogs of dsRNA and B-DNA (dsDNA of a right-handed spiral conformation), respectively, which could be recognized by several sensors, including TLR3, DNA-dependent activator of IRFs (DAI), etc. Reporter gene assays showed that US3 inhibited both poly(I·C) (Fig. 1E)- and poly(dA-dT) (Fig. 1F)-induced IFN-β promoter activity. Taken together, these results indicate that US3 is sufficient to inhibit SeV-mediated activation of IFN-β and ISRE promoter activities.

US3 inhibits IFN-β production by targeting IRF3. To determine at what level in the pathway US3 blocks IFN-β expression, we cotransfected increasing amounts of US3-expressing plasmids and expression plasmids of RIG-I-signaling pathway components, including the active caspase recruitment domain (CARD) containing a form of RIG-I (RIG-IN), mitochondrial antiviral signaling protein (MAVS), IKKε kinase, TBK1 kinase, and the active form of IRF3 (IRF3/5D) into HEK 293T cells. All expression constructs resulted in a 110- to 600-fold induction of (pRDIII-I)4-Luc reporter activity (Fig. 2A to E). PRD(III-I) promoter activation driven by all of the expression constructs was inhibited by US3 in a dose-dependent manner (Fig. 2A to E). Activation driven by RIG-IN, MAVS, or TBK1 was inhibited more than 90% (Fig. 2A to C), and activation driven by IKKε or IRF3/5D was inhibited up to 75% (Fig. 2D and E). These results indicate that US3 inhibits the IFN antiviral response at or downstream of IRF3.

IRF3 is a crucial transcription factor in the IFN-β-signaling pathway, and the dimerization of IRF3 is a hallmark of early activation of the antiviral response. To examine whether US3 affected IRF3 dimerization, we determined SeV-induced IRF3 dimerization in the presence or absence of US3. As shown in Fig. 2F, SeV infection induced the dimerization of IRF3, while US3 inhibited

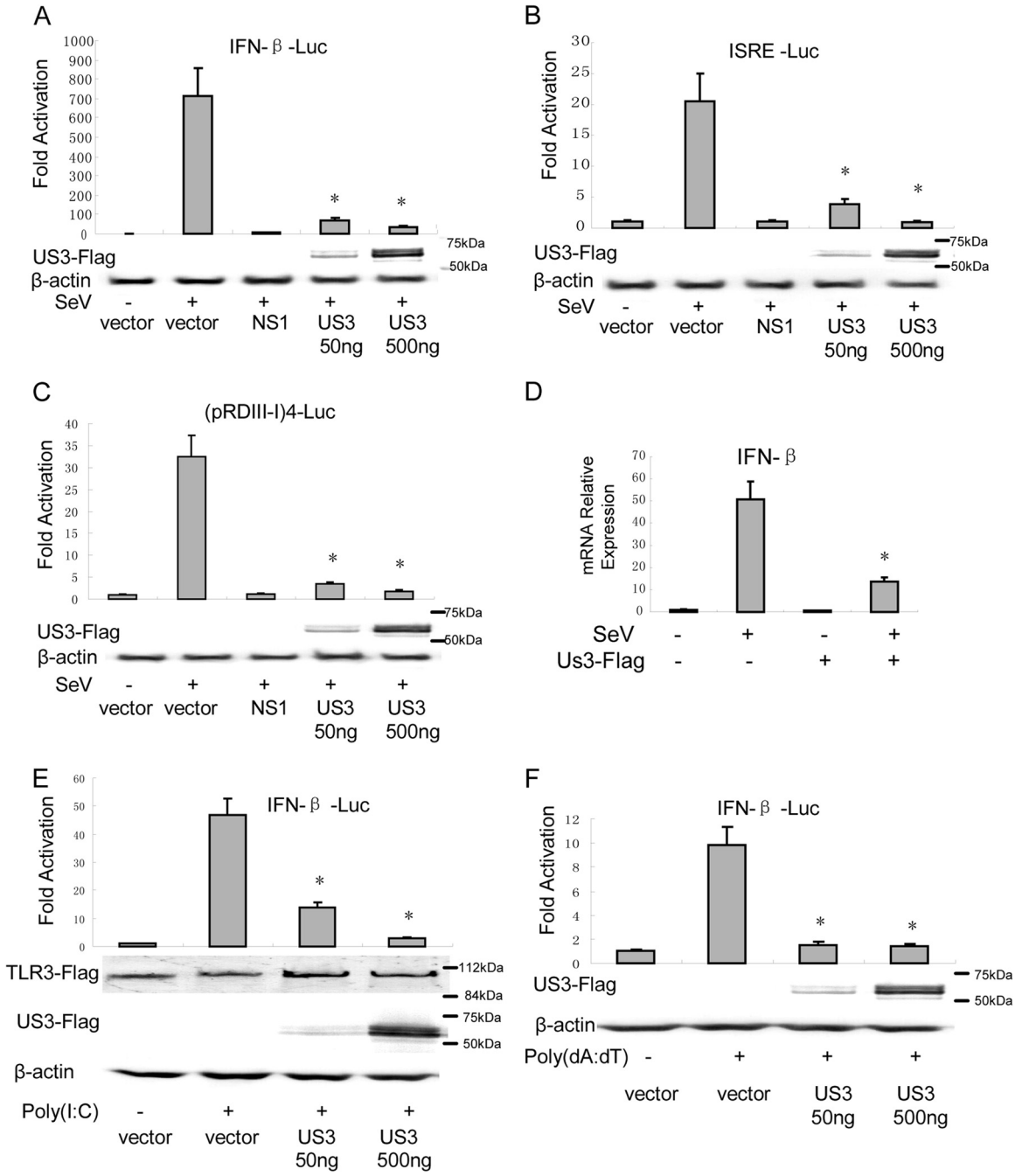

FIG 1 HSV-1 US3 inhibits IFN-β induction. HEK 293T cells were cotransfected with either IFN-β-Luc (A), ISRE-Luc (B), or (pRDIII-I)4-Luc (C) reporter plasmid along with pRL-TK control plasmid and empty vector or plasmids encoding the indicated viral proteins. Twenty-four hours after transfection, cells were infected with 100 HAU/ml of SeV or mock infected as indicated; luciferase activity was measured 16 h later, and fold activation was determined relative to that for empty vector with mock infection. (D) HEK 293T cells were transfected with Flag-US3 and infected with SeV as described for panel A. Real-time PCR analysis was then performed to detect the mRNA level of IFN-β. (E and F) US3 inhibited poly(I·C) (E)- and poly(dA-dT) (F)-induced IFN-β promoter activity. IFN-β-Luc, pRL-TK reporter plasmid, TLR3, and US3-expressing plasmid and empty vector were transfected as indicated. After 24 h, 100 ng/ml of poly(I·C) or poly(dA-dT) was transfected. Data are expressed as means and standard deviations from three independent experiments performed in duplicate. Statistical analysis was performed using the Student *t* test. *, $P < 0.05$.

SeV-mediated IRF3 dimerization. Taken together, these results indicate that US3 inhibits the IFN antiviral response by targeting IRF3.

The kinase activity of US3 is essential for inhibition of the IFN antiviral response. HSV-1 US3 is a viral Ser/Thr kinase. To determine whether the kinase activity of US3 is required for inhibition of the IFN antiviral response, we generated the kinase-dead (KD) US3 mutants K220M and D305A. Expression plasmids were cotransfected into HEK 293 cells and examined for their ability to inhibit SeV-induced IFN-β, PRD(III-I), and ISRE reporter gene

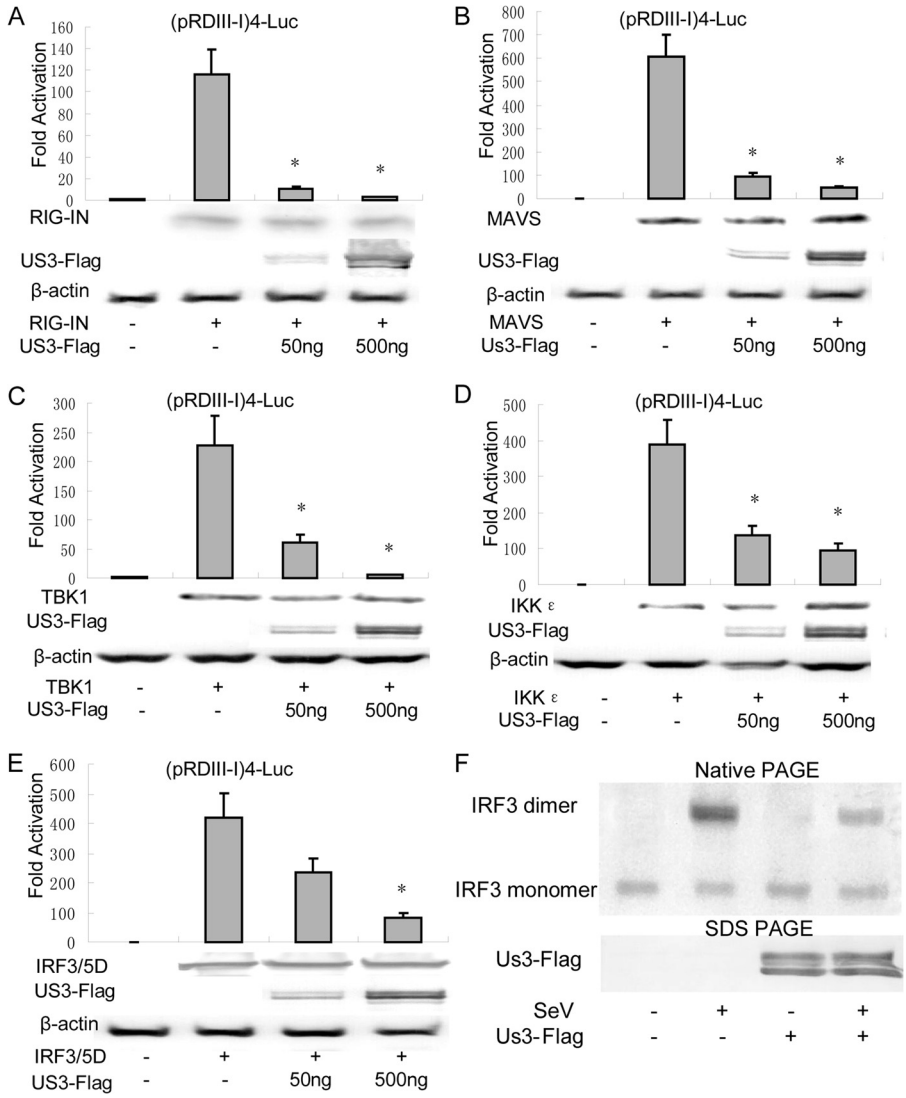

FIG 2 US3 targets IRF3 to inhibit IFN-β production. HEK 293T cells were cotransfected with (pRDIII-I)4-Luc reporter, PRL-TK, and RIG-IN (A), MAVS (B), TBK1 (C), IKKε (D), or IRF3/5D (E) expression plasmids along with the indicated amounts of US3 expression plasmid. Luciferase activity was analyzed as described in the legend to Fig. 1A. Data are means and standard deviations from three independent experiments performed in duplicate. Statistical analysis was performed using the Student *t* test. *, $P < 0.05$. (F) HEK 293T cells were transfected with the US3 expression plasmid. Twenty-four hours posttransfection, cells were mock infected or infected with 100 HAU/ml SeV for 8 h. Whole-cell extracts were subjected to native PAGE and probed with anti-IRF3 antibody to detect IRF3 dimerization.

activities. In agreement with the results shown in Fig. 1, Ectopic expression of wild-type US3 strongly inhibited SeV-mediated activation of IFN-β, PRD(III-I), and ISRE reporters. Ectopic expression of the K220M or D305A mutation failed to inhibit activation of SeV-induced IFN-β, PRD(III-I), and ISRE promoter activity (Fig. 3A). As determined by quantitative PCR, expression of wild-type US3 inhibited SeV-induced IFN-β, ISG54, and ISG56 mRNA expression, whereas the presence of both the K220M and D305A mutants had no significant effect (Fig. 3B). Furthermore, both the K220M and D305A mutants failed to inhibit SeV-mediated IRF3 dimerization, while US3 remarkably inhibited IRF3 dimerization, although a small part of the IRF3 dimer was detected due to transfection efficiency (Fig. 3C).

Nuclear translocation of IRF3 is crucial for the transcription of IFN-β. Immunofluorescence was carried out to investigate whether US3 prevented the nuclear translocation of IRF3 (Fig. 4). In mock-treated HeLa cells, IRF3 localized exclusively to the cytoplasm. SeV infection induced nuclear translocation of IRF3 in 97% of cells. Ectopic expression of US3 prevented the nuclear translocation of IRF3 induced by SeV infection in more than 80% of cells. However, the K220M and D305A mutants did not block the nuclear translocation of IRF3 (Fig. 4A and B). Therefore, these results demonstrate that the kinase activity of US3 is essential for US3-mediated inhibition of the IFN antiviral response.

US3 interacts with endogenous IRF3. Because US3 is a Ser/Thr kinase and the phosphorylation of IRF3 plays an important role in activation of the IFN antiviral response, we investigated the possibility that US3 interacts with and phosphorylates IRF3. In a co-IP assay, Flag-US3 expression plasmid was transfected into HEK 293T cells and the cells were subsequently infected with SeV.

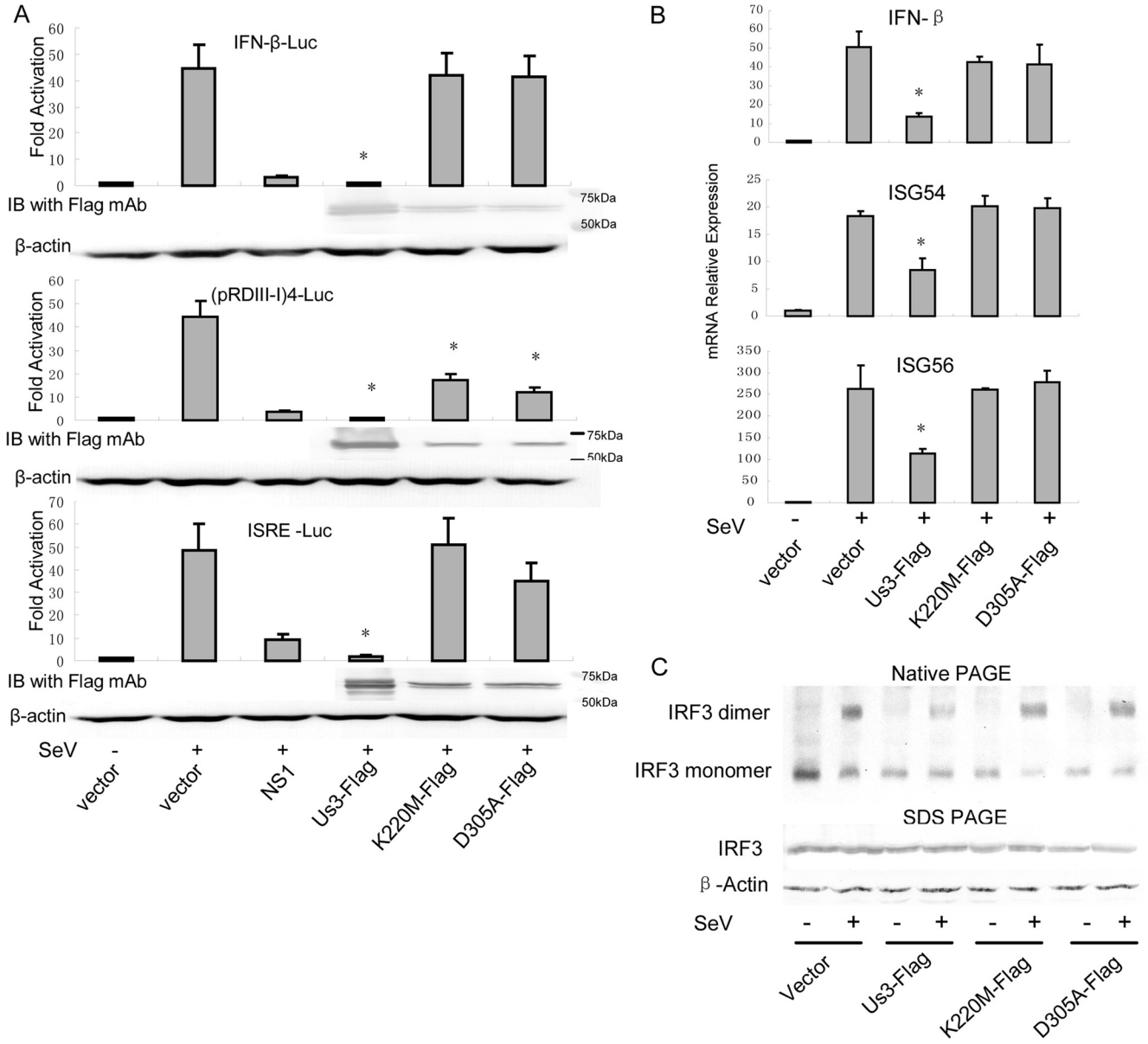

FIG 3 Kinase activity is required for US3-mediated inhibition of IFN-β production. (A) HEK 293T cells were cotransfected with PRL-TK plasmid and either IFN-β-Luc, (pRDIII-I)4-Luc, or ISRE-Luc reporter plasmid along with empty vector or plasmid encoding US3 WT, US3 K220M, or US3 D305A. Twenty-four hours posttransfection, cells were infected with 100 HAU/ml of SeV or mock-infected, and luciferase activity was analyzed as described in the legend to Fig. 1A. IB, immunoblot. (B and C) HEK 293T cells were transfected with empty vector or plasmid encoding US3 WT, US3 K220M, or US3 D305A. Twenty-four hours posttransfection, cells were infected with 100 HAU/ml of SeV or mock-infected for 16 h. (B) Quantitative PCR analysis was performed to detect the mRNA levels of IFN-β, ISG54, and ISG56. Data are means and standard deviations from three independent experiments. Statistical analysis was performed using the Student *t* test. *, $P < 0.05$. (C) Native PAGE assays were performed to detect IRF3 dimerization as described in the legend to Fig. 2F.

Endogenous IRF3 was efficiently coimmunoprecipitated by Flag mouse monoclonal antibody but not by the nonspecific antibody IgG2b (Fig. 5A). In order to investigate the interaction between US3 and IRF3 in the context of HSV-1 infection, we generated a US3-Flag HSV-1, that is, a Flag tag in frame with the C terminus of US3, with the BAC recombinant system developed in our lab (Fig. 5B) (60, 61). The HSV-1 BAC contains a firefly luciferase cassette, and the luciferase activity could be easily quantified *in vitro*. Luciferase activity assays were used to determine the replication kinetics of US3-Flag mutant HSV-1 and WT HSV-1 (Fig. 5C and D). The results showed that US3-Flag mutant HSV-1 replicated as efficiently as WT HSV-1 in both HEK 293T cells (Fig. 5C) and Vero cells (Fig. 5D). Furthermore, WB assays showed similar expression of UL42 and UL46 in US3-Flag mutant HSV-1- and WT HSV-1-infected HEK 293T cells (Fig. 5E). WB assays detected the expression of US4 in US3-Flag mutant HSV-1-infected Vero cells, suggesting that the insertion of the Flag sequence in the 3′-terminal end of US3 did not affect the promoter of US4 (data not shown). Quantitative PCR showed that only a trace amount of IFN-β transcription was detected in WT HSV-1- or US3-Flag mutant HSV-1-infected HEK 293 cells, implying that US3-Flag mutant HSV-1 has the same ability as WT HSV-1 to inhibit IFN-β

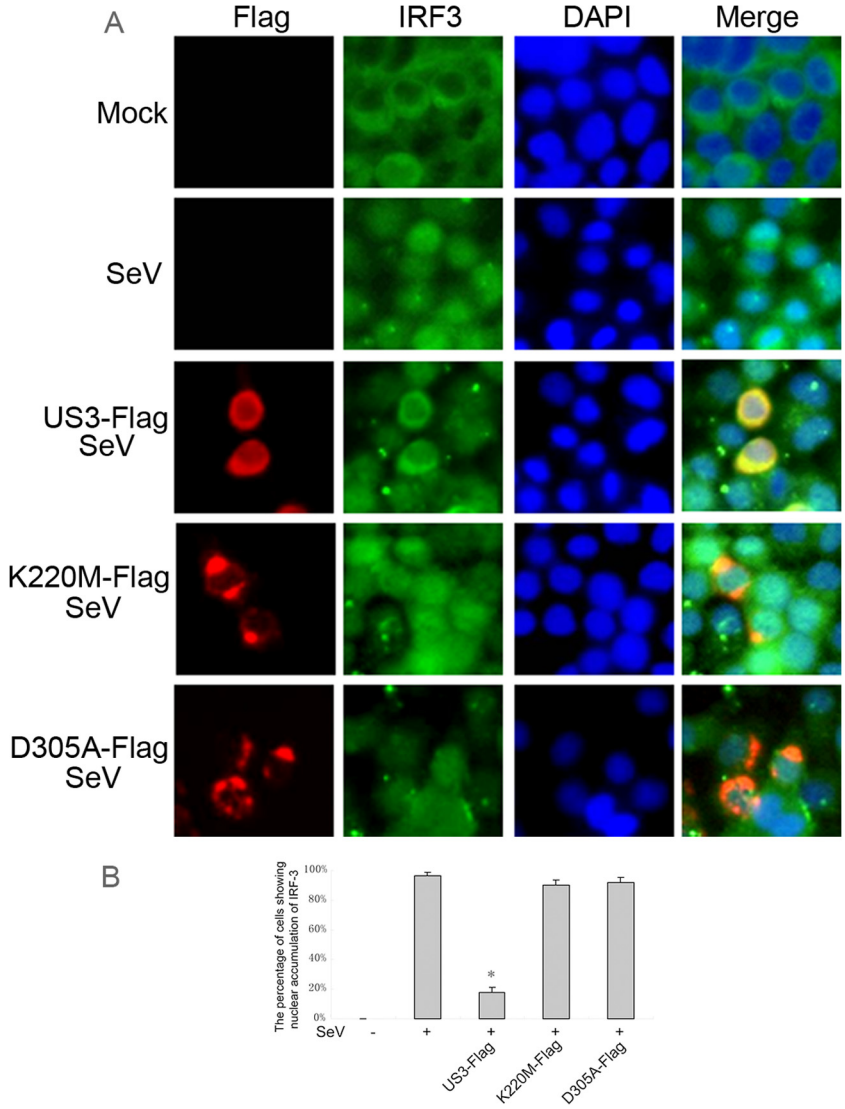

FIG 4 US3 blocks SeV-induced IRF3 nuclear translocation. (A) HeLa cells were transfected with empty vector, Flag-tagged US3 WT, US3 K220M, or US3 D305A expression plasmid. Twenty-four hours posttransfection, cells were infected with 100 HAU/ml of SeV or mock-infected for 8 h as indicated. Cells were stained with mouse anti-Flag MAb and rabbit anti-IRF3 pAb. FITC-conjugated goat anti-rabbit (green) and TRITC-conjugated goat anti-mouse (red) were used as the secondary antibodies. Cell nuclei (blue) were stained with Hoechst 33258. The images were obtained by fluorescence microscopy using a 40× lens objective. (B) Statistical analysis of the percentage of cells exhibiting nuclear accumulation of IRF3 in panel A. Statistical analysis was performed using the Student *t* test. *, $P < 0.05$.

production (Fig. 5F). Subsequently, HEK 293T cells were infected with the recombinant virus US3-Flag mutant HSV-1 at an MOI of 1 for 20 h, and US3-Flag-fused protein could be detected by Flag MAb. As expected, endogenous IRF3 could also be coimmunoprecipitated by Flag MAb (Fig. 5G). Also, co-IP was carried out to determine whether the K220M and D305A mutants abrogated their interaction with IRF3 and failed to inhibit IFN-β production. Both US3 mutants still interacted with IRF3, confirming that the kinase activity of US3 is required for US3-mediated inhibition of IFN-β production (Fig. 5H).

US3 phosphorylates IRF3 at the site of Ser175. The aforementioned data have demonstrated that US3 interacts with IRF3 and that the kinase activity is required for US3-mediated inhibition of the IFN antiviral response. We speculated that IRF3 might serve as a substrate of US3 protein kinase. To test this hypothesis, we transfected HEK 293T cells with wild-type and KD mutants of US3 expression plasmids infected with SeV and subjected them to WB analysis. The results indicated that expression of US3 induced an additional slowly migrating form of IRF3 (Fig. 6A, lanes 3 and 5). To determine whether the slowly migrating forms of IRF3 were due to US3-induced hyperphosphorylation, we subjected the different forms of IRF3 to treatment *in vitro* with calf intestine alkaline phosphatase (CIP). The slowly migrating form of IRF3 completely disappeared following CIP treatment (Fig. 6A, lanes 4 and 6), indicating that the slowly migrating forms of IRF3 were hyperphosphorylated IRF3. Hyperphosphorylation of IRF3 was detected in both SeV-infected and uninfected cells (Fig. 6A, lanes 3 and 5), suggesting that the hyperphosphorylation of IRF3 by US3 was independent of SeV infection. The KD mutants K220M and D305A were unable to hyperphosphorylate IRF3 (Fig. 6A, lanes 7

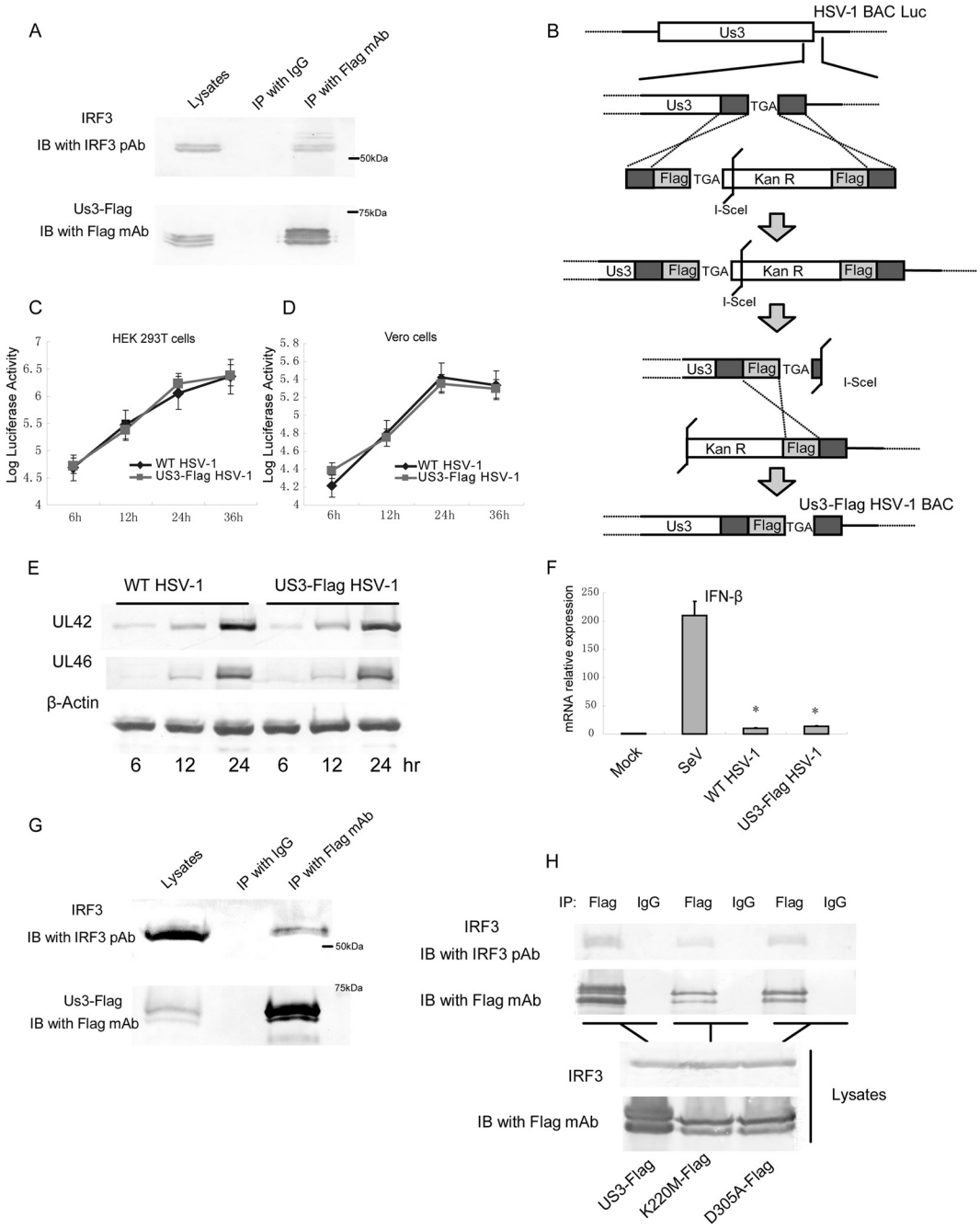

FIG 5 US3 interacts with IRF3. (A) HEK 293T cells were transfected with Flag-tagged US3 plasmid. Twenty-four hours posttransfection, cells were infected with SeV. Flag-tagged US3 was immunoprecipitated (IP) using an anti-FLAG antibody or nonspecific mouse antibody IgG2b (control) and subjected to immunoblot (IB) analysis using an anti-IRF3 antibody to detect endogenous IRF3 interaction. (B) Schematic diagram of the construction of US3-Flag HSV-1. A Flag tag was inserted into the C terminus of US3 in the HSV-1 genome. Confluent HEK 293T cells (C and E) or Vero cells (D) were infected with the indicated viruses at an MOI of 0.1. Growth curves were generated by luciferase activity assays (C and D), and expression of UL42 and UL46 was detected by WB assays (E). (F) HEK 293T cells were infected with WT HSV-1 or US3-Flag HSV-1 for 16 h, and quantitative PCR assays were performed to detect the mRNA levels of IFN-β. Statistical analysis was performed using the Student *t* test. *, $P < 0.05$. (G) HEK 293T cells were infected with US3-Flag HSV-1 at an MOI of 5 for 20 h. Co-IP assays were performed to investigate the interaction between endogenous IRF3 and US3. (H) HEK 293T cells were transfected with Flag-tagged US3, US3 K220M, or US3 D305A plasmid. Twenty-four hours posttransfection, co-IP assays were performed to detect the interaction between endogenous IRF3 and US3 K220M or US3 D305A.

and 8). WB analysis with IRF3 Ser396 phospho-specific antibody demonstrated that US3 did not affect SeV-mediated Ser396 phosphorylation of IRF3 (Fig. 6A, middle panel, lane 5). Furthermore, US3 did not induce the typical phosphorylation of IRF3 at the Ser396 site (Fig. 6A, lane 3). To confirm this result, we coexpressed Flag-US3 with a Myc-tagged truncated form of IRF3 (Myc-IRF3 1-394), which lacks the typical phosphorylation site Ser396 (Fig. 6B). WB analysis showed that US3 hyperphosphorylated trun-

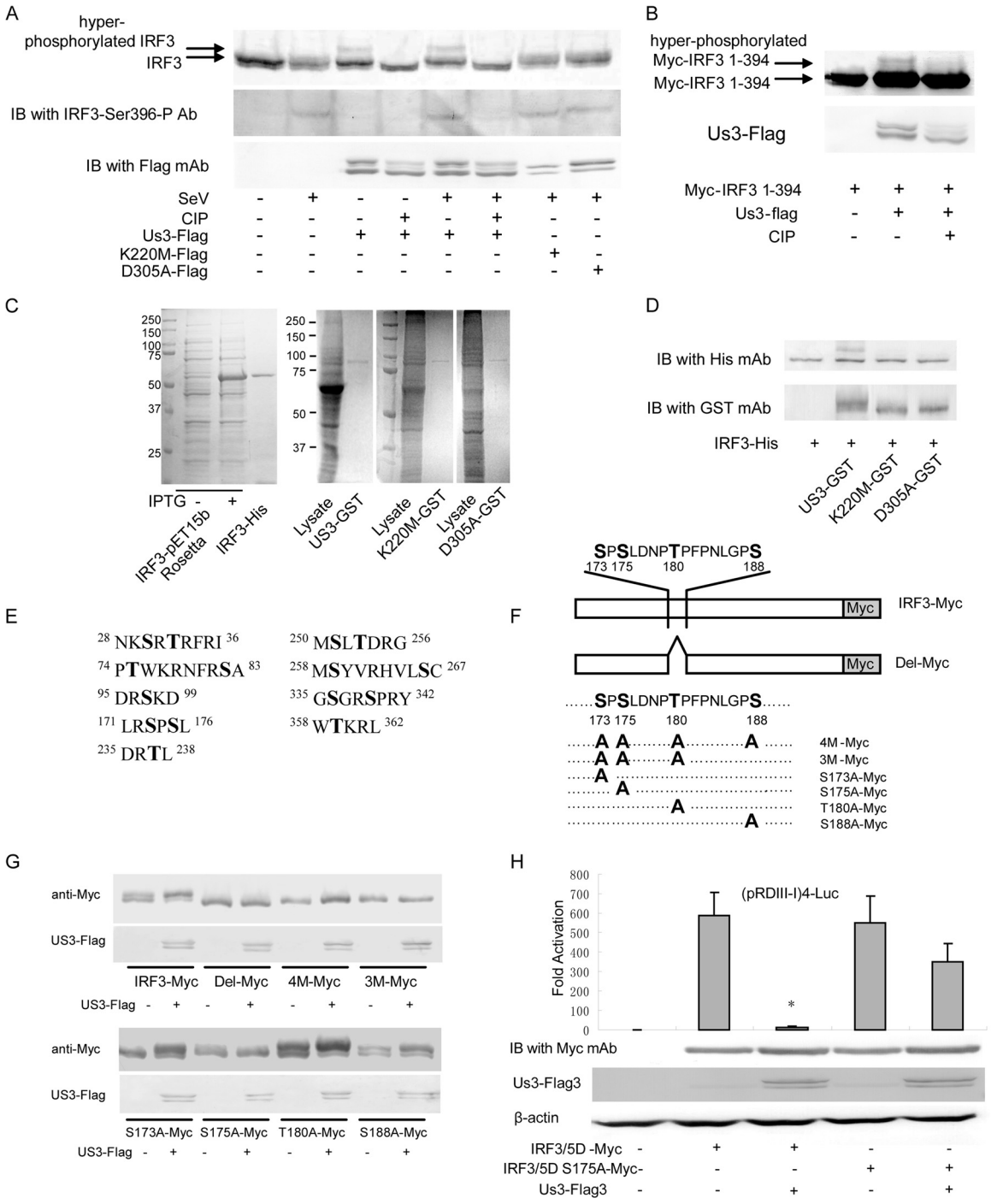

FIG 6 US3 hyperphosphorylates IRF3 at Ser175. (A) HEK 293T cells were transfected with Flag-tagged US3 WT, US3 K220M, or US3 D305A expression plasmid as indicated. Twenty-four hours posttransfection, cells were infected or not infected with SeV for 8 h. Whole-cell extracts were prepared, treated or not treated with CIP for 1 h, as indicated, and subjected to immunoblot analysis for phosphorylated IRF3 (Ser396), IRF3, and US3-Flag. IRF3-Ser396-P Ab, phospho-specific antibody against phosphorylated IRF3 (Ser396). (B) HEK 293T cells were transfected with Myc-IRF3 (1 to 394) alone or together with Flag-tagged US3 as indicated. Twenty-four hours posttransfection, whole-cell extracts were prepared, treated or not treated with CIP for 1 h, and subjected to WB analysis using anti-Myc and anti-Flag antibodies. (C) SDS-PAGE analysis of the expressed IRF3-His in *E. coli* and US3-GST, K220M-GST, and D305A-GST in HEK 293T cells. (D) A protein kinase assay was performed with purified IRF3-His and US3-GST, K220M-GST, D305A-GST, and WB assays were subsequently performed with anti-His and anti-GST antibodies. (E) Predicted IRF3 phosphorylation sites targeted by US3. (F) Schematic diagram of a series of IRF3 mutants used for Fig. 5G. (G) A series of IRF3 mutants were cotransfected with or without US3-Flag plasmid. Twenty-four hours posttransfection, cell lysates were subjected to WB analysis. (H) The plasmid IRF3/5D with mutant S175A was subjected to DLR assays as described in the legend to Fig. 2E. US3 did not inhibit IRF3/5D S175A-mediated reporter activity. Statistical analysis was performed using the Student *t* test. *, $P < 0.05$.

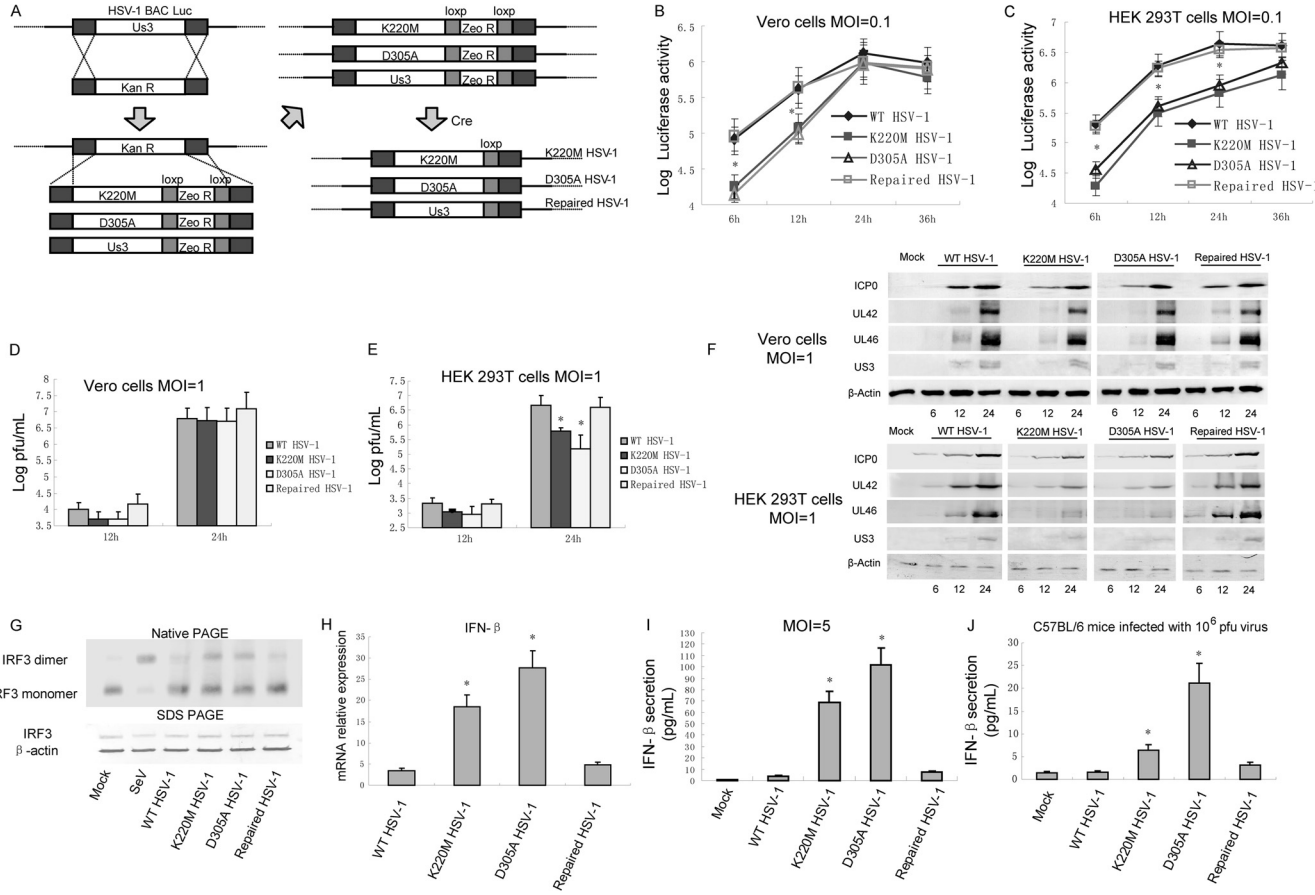

FIG 7 US3 KD mutant HSV-1 induced more IFN-β production than WT HSV-1. (A) Schematic diagram of the construction of K220M and D305A mutant HSV-1 and repaired HSV-1. Confluent Vero cells (B and D) or HEK 293T cells (C and E) were infected with the indicated viruses at MOIs of 0.1 (B and C) or 1 (D and E). Growth curves were generated by luciferase activity assays (B and C) and traditional plaque assays (D and E). (F) Protein expression levels of UL42, UL46, and US3 were detected by WB assays. (G) HEK 293T cells were infected with the indicated viruses at an MOI of 5. Twenty hours postinfection, cellular lysates were subjected to native PAGE and probed with anti-IRF3 antibody to detect the IRF3 dimer. (H) HEK 293T cells were infected with the indicated virus for 10 h, and quantitative PCR assays were performed to detect the mRNA levels of IFN-β. (I) HEK 293T cells in a 24-cell plate were infected with WT, K220M or D305A mutant, or repaired HSV-1 at an MOI of 5 for 20 h. Media from the infected cells were analyzed by ELISA for IFN-β secretion. (J) C57BL/6 mice were intraperitoneally infected with 10^6 PFU of the indicated virus. After 24 h, serum were collected and subjected to ELISA to detect IFN-β production. The data represent means plus standard deviations for three replicates. Statistical analysis was performed using the Student *t* test. *, $P < 0.05$.

cated IRF3, indicating that the phosphorylation sites of IRF3 induced by US3 are located between amino acids 1 and 394. Furthermore, we examined whether US3 phosphorylated IRF3 directly. His-tagged IRF3 (IRF3-His) was expressed in *E. coli* Rosetta cells and purified with His-Bind resin (Novagen). GST-tagged US3, K220M, or D305A (US3-GST, K220M-GST, or D305A-GST) was expressed in HEK 293T cells and purified with GST resin (Fig. 6C). The purified proteins were subjected to protein kinase assay, and a slowly migrating form of IRF3-His was detected by WB assay when IRF3-His incubated with US3-GST but not when it was incubated with K220M-GST or D305A-GST (Fig. 6D). These results indicate that US3 phosphorylates IRF3 directly *in vitro*.

US3 usually targets Ser or Thr residues within motifs containing Arg or Lys. However, there were 9 predicted sites in IRF3, and it was hard to determine the phosphorylation sites by mutation analysis (Fig. 6E). In order to identify the hyperphosphorylation sites in IRF3 by US3, we cotransfected plasmids expressing Myc-tagged IRF3 and US3-Flag into HEK 293T cells, immunoprecipitated IRF3-Myc by Myc MAb, and subjected it to SDS-PAGE. The band of hyperphosphorylated IRF3 was cut and subjected to mass spectrometry to identify the hyperphosphorylation site of IRF3. Peptide ^{173}SPSLDNPTPFPNLGPSENPLKR^{194} containing the Ser/Thr phosphorylation site was found to be the substrate of US3. A series of IRF3 mutants were constructed to identify the exact IRF3 hyperphosphorylation amino acids (Fig. 6F). As shown in Fig. 6G, mutants of Del-Myc (Ser173 to Ser188 deleted), 4 M-Myc (Ser173, Ser175, Thr180, and S188 all mutated into Ala) and 3 M-Myc (Ser173, Ser175, and Thr180 mutated into Ala) could not be hyperphosphorylated by US3. Subsequently, we tested the single-point mutant and found that only the S175A mutant abolished hyperphosphorylation by US3. A plasmid of IRF3/5D harboring the S175A mutant was generated and subjected to DLR assay. The results show that both IRF3/5D and IRF3/5D S175A induced more than 500-fold of (pRDIII-I)4-Luc reporter activity. US3 significantly inhibited IRF3/5D- but not IRF3/5D S175A-mediated reporter activity, confirming that US3 hyperphosphorylated IRF3 at Ser175 (Fig. 6H). Taken

together, our data strongly demonstrate that US3 protein kinase interacts with IRF3 and hyperphosphorylates IRF3 at an atypical site of Ser175.

US3 KD mutant virus induced a larger amount of IFN-β than WT virus. To investigate the physiological functions of US3 in the context of HSV-1 infection, we generated both US3 K220M and D305A mutants of HSV-1 and repaired HSV-1 using our HSV-1 BAC system as previously described (Fig. 7A) (60). US4 was detected in all of the recombinant-virus-infected cells, suggesting that the insertion of the *loxP* sequence did not disturb the US4 promoter (data not shown). Luciferase activity assays were used to determine the replication kinetics of the HSV-1 mutants and WT HSV-1 in both Vero cells (Fig. 7B) and HEK 293T cells (Fig. 7C). Both the K220M and D305A mutants only slightly delayed viral replication compared with WT HSV-1 and repaired HSV-1 when the cells were infected with the corresponding viruses at an MOI of 0.1 (Fig. 7B). Because the Vero cells are devoid of an IFN response, replication kinetics in HEK 293T cells were also generated by luciferase activity assays. Interestingly, replication of the K220M mutant and HSV-1 decreased significantly compared with replication of WT and repaired viruses (Fig. 7C). Traditional plaque assays were also performed at an MOI of 1, and the results correlated with luciferase activity (Fig. 7D and E). To confirm the different replication of US3 KD viruses in Vero cells and HEK 293T cells, we performed WB assays to detect the expression of ICP0, UL42, UL46, and US3. The results showed that the K220M and D305A mutants remarkably decreased the expression of ICP0, UL42, UL46, and US3 in HEK 293T cells but not in Vero cells, confirming the results of the replication kinetics assay (Fig. 7F). Subsequently, native PAGE assays were performed to investigate IRF3 dimerization after infection by recombinant viruses. SeV infection served as the positive control and resulted in a high level of IRF3 dimer. Infection by WT HSV-1 and repaired HSV-1 caused only trace amounts of IRF3 dimer. Compared with that in WT HSV-1 and repaired-HSV-1 infections, a higher level of IRF3 dimer was detected after infection with K220M mutant or D305A mutant HSV-1 (Fig. 7G). Quantitative PCR was performed to measure IFN-β mRNA expression in HEK 293 cells infected with wild-type or mutant virus at an MOI of 5 for 10 h. The WT HSV-1 and repaired-HSV-1 infections only slightly upregulated IFN-β transcription. Both the K220M and D305A mutant viruses induced significantly higher levels of IFN-β mRNA than WT HSV-1 did (Fig. 7H). ELISAs were also performed to measure the secretion of IFN-β when cells were infected with these viruses at an MOI of 5 for 10 h. The results indicated that both K220M and D305A mutant HSV-1 induced significantly higher levels of IFN-β secretion than WT and repaired HSV-1 (Fig. 7H). In addition, C57BL/6 mice were infected with 10^6 PFU of the WT, K220M, D305A, or repaired HSV-1 for 24 h, and serum IFN-β was detected with ELISA kits. WT HSV-1 and repaired HSV-1 induced only a small amount of IFN-β. K220M and D305A mutant HSV-1 infections induced about 6 and 21 ng/ml of IFN-β, respectively, which was remarkable higher than that induced by WT and repaired-virus infections (Fig. 7I).

Taken together, these pieces of evidence demonstrate that HSV-1 US3 interacts with and hyperphosphorylates IRF3 at Ser175, contributing to the abrogation of IFN-β production and immune evasion during HSV-1 infection.

DISCUSSION

The innate immune response serves as the first line of host defense against virus infection. The IFN-β-signaling pathway is one of the most important mechanisms to eliminate viral infection. TLR3, RIG-I, and MDA-5 recognize viral dsRNA, a by-product of virus replication. These receptors recruit adaptor proteins and subsequently activate the transcription factors IRF3 and NF-κB. Activated IRF3 translocates to the nuclei and then binds to PRDIII-I of the IFN-β promoter, inducing synthesis of IFN-β (63, 64).

HSV-1 US3 has been previously reported to be a potent inhibitor of the IFN response, serving as one of several strategies by HSV-1 to interrupt the innate immune system. It has been reported that infection with US3-null HSV-1 increased IRF3 activation and TLR3 and IFN levels in infected monocytic cells (41). However, the molecular mechanism remains unclear. In this study, US3 was proven to significantly inhibit SeV-induced activation of the IFN-β and ISRE promoter. DLR assays showed that US3 inhibited RIG-IN-, MAVS-, TBK1-, IKKε-, and IRF3/5D-mediated activation of the PRDIII-I promoter. Subsequently, US3 was shown to abrogate the dimerization and nuclear localization of IRF3. Colocalization of US3 with endogenous IRF3 suggested interaction between US3 and IRF3, which was validated by co-IP assay. The more slowly migrating forms of hyperphosphorylated IRF3 were detected in US3-transfected cells and were sensitive to CIP treatment. Subsequently, we proved that US3 hyperphosphorylated IRF3 at Ser175. Thus, our results demonstrate that HSV-1 US3 interacts with and hyperphosphorylates IRF3 to abolish the dimerization and nuclear translocation of IRF3 and the production of IFN-β.

HSV-1 US3 protein kinase and its orthologues have a kinase domain containing the ATP binding domain and the catalytic active site. K220 of HSV-1 US3 is critical for ATP binding, and D305 is critical for catalytic activity (65). The K220M and D305A mutants did not hyperphosphorylate IRF3, and neither of them prevented the dimerization and nuclear localization of IRF3 or inhibited SeV-induced IFN-β production, indicating that the KD mutants abolished the inhibitory activity. However, either the K220M or the D305A mutant still slightly inhibited SeV-induced PRD(III-I) promoter activity, as shown in Fig. 3A, suggesting that the interaction between the KD mutants and IRF3 might slightly interfere with the IRF3 activity. Moreover, both the K220M and D305A mutant HSV-1 induced more IFN-β production than WT HSV-1 and repaired virus. All these results indicate that the kinase activity of US3 is required for its inhibitory activity against IFN-β production.

US3 protein kinase was reported to enhance viral-gene expression by masquerading as the cellular kinase Akt to phosphorylate TSC2 and inhibit the translational repressor 4E-BP1 (24, 25). In our study, US3 KD mutant viruses showed only delayed replication in Vero cells. Given the fact that Vero cells are deficient in the IFN response, the delayed replication may result mainly from the inability of the US3 mutant to promote viral-protein expression. Interestingly, the replication of K220M mutant HSV-1 and D305A mutant HSV-1 remarkably decreased by about 1 log in HEK 293T cells compared with replication of WT and repaired HSV-1, confirming a previous study from another lab (5). We deduced that the decreased replication of US3 KD viruses results from loss of function of both the enhancement of viral-protein expression and immune evasion by US3.

HSV-1 is a highly successful human pathogen. Although the immune response to HSV-1 is complicated, a number of HSV-1 proteins, including ICP0 (29), ICP34.5 (30), US3 (41), ICP27 (35), Vhs (32), US11 (36), VP16 (37), etc., contribute to immune evasion by HSV-1 through multiple different mechanisms. All these proteins may function cooperatively; deletion of one of these proteins would increase IFN-β production to a certain extent. Although K220M and D305A mutant HSV-1 induced higher levels of IFN-β production, IFN-β production in US3 KD mutant HSV-1-infected cells was still much lower than that in SeV-infected cells, suggesting that other HSV-1 proteins also contributed to the downregulation of IFN-β production. Thus, we inferred that US3 functioned cooperatively with other proteins to inhibit IFN-β production.

IRF3 plays a crucial role in IFN-β production because all signals converge at IRF3 or IRF7. Thus, viruses are more likely to evolve strategies, such as varicella-zoster virus (VZV) ORF61 (44), VZV ORF47 (66), the severe acute respiratory coronavirus (SARS-CoV) papain-like protease domain (67), human bocavirus NP1 (68), etc., to counteract innate immunity by targeting IRF3. Besides US3, HSV-1 ICP0 was demonstrated to inhibit the production of IFN-β by sequestrating IRF3; the ICP0 mutant virus induced an enhanced innate antiviral response (29, 69). ICP0 is an immediate early protein and capable of transactiving the early and late genes of HSV-1, so ICP0 mutant HSV-1 will definitely decrease the expression of the early and late genes and mask the actual immune evasion function of other genes, such as US3, and the aforementioned viral proteins.

Previous studies reported that US3 kinases from HSV-1 and other alphaherpesviruses and pseudorabies virus (PRV) show a similar minimal consensus phosphorylation sequence, which was characterized as (R)n-X-(S/T)-Z-Z ($n \geq 2$; X can be absent or Arg, Ala, Val, Pro, or Ser; Z can be any amino acid except Pro or an acidic residue) (70, 71). It was also reported that US3 protein kinases phosphorylated the same substrates as protein kinase A (PKA) (65, 72). Recently it was determined that HSV-1 US3 can masquerade as Akt and phosphorylate the same substrates as Akt (24). It has been previously reported that VZV ORF66 directly phosphorylates IE62 at the nuclear localization signal of IE62, which is sufficient to regulate IE62 nuclear import (73). In this study, US3 has been shown to inhibit the nuclear translocation of IRF3; accordingly, we speculated that US3 phosphorylates IRF3 at the nuclear location signal of IRF3 (amino acid region 70 to 92) (74). However, mass spectrometry and WB analysis showed that US3 hyperphosphorylated IRF3 at Ser175, suggesting that the substrates of US3 are more complicated than expected. Native PAGE showed that US3 inhibited the dimerization of IRF3, which further led to inhibition of the nuclear translocation of IRF3. Ser175 located in the region between the DNA binding and IRF association domains of IRF3, which might be a preferred target for viral kinase. Epstein-Barr virus BGLF4 kinase suppresses the IRF3-mediated pathway by phosphorylating IRF3 at Ser123, Ser173, and Thr180 (75), two of which are also in this region. The VZV ORF47 was also reported to phosphorylate IRF3 and inhibit IFN-β production (66). However, the phosphorylation site of IRF3 by ORF47 has not yet been identified and warrants further investigation.

HSV-1 US3 was also reported to play a role in the inhibition of a subsequent IFN-mediated signaling pathway. US3-null HSV-1 was more sensitive than WT HSV-1 to IFN-α (39). US3 protein kinase was also demonstrated to block IFN-γ-induced ISG expression by phosphorylating the alpha subunit of the IFN-γ receptor (40). DLR assays also showed that transfection of US3 significantly inhibits ISRE promoter activity. All of these facts suggest that HSV-1 US3 suppresses innate antiviral immunity through multiple mechanisms at multiple levels of innate signaling pathways.

Taken together, our results provide further information on the mechanism by which HSV-1 US3 antagonizes the host innate antiviral response. We have shown convincing evidence that HSV-1 US3 protein kinase inhibits the IFN-β-signaling pathway by interacting with and hyperphosphorylating IRF3. Our results expand our knowledge about the molecular mechanisms by which HSV-1 counteracts host innate antiviral immunity to ensure its replication and spread.

ACKNOWLEDGMENTS

This work was supported by the National Natural Science Foundation of China (81171584), the Program for Changjiang Scholars and Innovative Research Team in Soochow University (PCSIRT, IRT1075), and the Jiangsu Provincial Innovative Research Team.

We thank Yi-Ling Lin for the gift of plasmid IRF3/5D, S. Ludwig for (pRDDIII-)4-Luc, Greg Smith for GS1783, and Takashi Fujita for pEF-Flag-RIG-IN, pMyc-MAVS, and IFN-β-Luc. We thank You Li for help with construction of HSV-1 KD mutant viruses.

REFERENCES

1. **Kadowaki N, Antonenko S, Lau JY, Liu YJ.** 2000. Natural interferon alpha/beta-producing cells link innate and adaptive immunity. J. Exp. Med. **192:**219–226.
2. **Randall RE, Goodbourn S.** 2008. Interferons and viruses: an interplay between induction, signalling, antiviral responses and virus countermeasures. J. Gen. Virol. **89:**1–47.
3. **Sarkar SN, Sen GC.** 2004. Novel functions of proteins encoded by viral stress-inducible genes. Pharmacol. Ther. **103:**245–259.
4. **Takeuchi O, Akira S.** 2009. Innate immunity to virus infection. Immunol. Rev. **227:**75–86.
5. **Reynolds AE, Wills EG, Roller RJ, Ryckman BJ, Baines JD.** 2002. Ultrastructural localization of the herpes simplex virus type 1 UL31, UL34, and US3 proteins suggests specific roles in primary envelopment and egress of nucleocapsids. J. Virol. **76:**8939–8952.
6. **Wagenaar F, Pol JM, Peeters B, Gielkens AL, de Wind N, Kimman TG.** 1995. The US3-encoded protein kinase from pseudorabies virus affects egress of virions from the nucleus. J. Gen. Virol. **76:**1851–1859.
7. **Mou F, Forest T, Baines JD.** 2007. US3 of herpes simplex virus type 1 encodes a promiscuous protein kinase that phosphorylates and alters localization of lamin A/C in infected cells. J. Virol. **81:**6459–6470.
8. **Imai T, Arii J, Minowa A, Kakimoto A, Koyanagi N, Kato A, Kawaguchi Y.** 2011. Role of the herpes simplex virus 1 Us3 kinase phosphorylation site and endocytosis motifs in the intracellular transport and neurovirulence of envelope glycoprotein B. J. Virol. **85:**5003–5015.
9. **Asano S, Honda T, Goshima F, Watanabe D, Miyake Y, Sugiura Y, Nishiyama Y.** 1999. US3 protein kinase of herpes simplex virus type 2 plays a role in protecting corneal epithelial cells from apoptosis in infected mice. J. Gen. Virol. **80:**51–56.
10. **Leopardi R, Van Sant C, Roizman B.** 1997. The herpes simplex virus 1 protein kinase US3 is required for protection from apoptosis induced by the virus. Proc. Natl. Acad. Sci. U. S. A. **94:**7891–7896.
11. **Cartier A, Komai T, Masucci MG.** 2003. The Us3 protein kinase of herpes simplex virus 1 blocks apoptosis and induces phosporylation of the Bcl-2 family member Bad. Exp. Cell Res. **291:**242–250.
12. **Benetti L, Roizman B.** 2007. In transduced cells, the US3 protein kinase of herpes simplex virus 1 precludes activation and induction of apoptosis by transfected procaspase 3. J. Virol. **81:**10242–10248.
13. **Geenen K, Favoreel HW, Olsen L, Enquist LW, Nauwynck HJ.** 2005. The pseudorabies virus US3 protein kinase possesses anti-apoptotic activity that protects cells from apoptosis during infection and after treatment with sorbitol or staurosporine. Virology **331:**144–150.
14. **Hata S, Koyama AH, Shiota H, Adachi A, Goshima F, Nishiyama Y.**

1999. Antiapoptotic activity of herpes simplex virus type 2: the role of US3 protein kinase gene. Microbes Infect. **1:**601–607.
15. **Ogg PD, McDonell PJ, Ryckman BJ, Knudson CM, Roller RJ.** 2004. The HSV-1 Us3 protein kinase is sufficient to block apoptosis induced by overexpression of a variety of Bcl-2 family members. Virology **319:**212–224.
16. **Favoreel HW, Van Minnebruggen G, Adriaensen D, Nauwynck HJ.** 2005. Cytoskeletal rearrangements and cell extensions induced by the US3 kinase of an alphaherpesvirus are associated with enhanced spread. Proc. Natl. Acad. Sci. U. S. A. **102:**8990–8995.
17. **Van den Broeke C, Radu M, Deruelle M, Nauwynck H, Hofmann C, Jaffer ZM, Chernoff J, Favoreel HW.** 2009. Alphaherpesvirus US3-mediated reorganization of the actin cytoskeleton is mediated by group A p21-activated kinases. Proc. Natl. Acad. Sci. U. S. A. **106:**8707–8712.
18. **Finnen RL, Roy BB, Zhang H, Banfield BW.** 2010. Analysis of filamentous process induction and nuclear localization properties of the HSV-2 serine/threonine kinase Us3. Virology **397:**23–33.
19. **Morimoto T, Arii J, Tanaka M, Sata T, Akashi H, Yamada M, Nishiyama Y, Uema M, Kawaguchi Y.** 2009. Differences in the regulatory and functional effects of the Us3 protein kinase activities of herpes simplex virus 1 and 2. J. Virol. **83:**11624–11634.
20. **Poon AP, Gu H, Roizman B.** 2006. ICP0 and the US3 protein kinase of herpes simplex virus 1 independently block histone deacetylation to enable gene expression. Proc. Natl. Acad. Sci. U. S. A. **103:**9993–9998.
21. **Walters MS, Kinchington PR, Banfield BW, Silverstein S.** 2010. Hyperphosphorylation of histone deacetylase 2 by alphaherpesvirus US3 kinases. J. Virol. **84:**9666–9676.
22. **Jung M, Finnen RL, Neron CE, Banfield BW.** 2011. The alphaherpesvirus serine/threonine kinase Us3 disrupts promyelocytic leukemia protein nuclear bodies. J. Virol. **85:**5301–5311.
23. **Rao P, Pham HT, Kulkarni A, Yang Y, Liu X, Knipe DM, Cresswell P, Yuan W.** 2011. Herpes simplex virus 1 glycoprotein B and US3 collaborate to inhibit CD1d antigen presentation and NKT cell function. J. Virol. **85:**8093–8104.
24. **Chuluunbaatar U, Roller R, Feldman ME, Brown S, Shokat KM, Mohr I.** 2010. Constitutive mTORC1 activation by a herpesvirus Akt surrogate stimulates mRNA translation and viral replication. Genes Dev. **24:**2627–2639.
25. **Chuluunbaatar U, Mohr I.** 2011. A herpesvirus kinase that masquerades as Akt: you don't have to look like Akt, to act like it. Cell Cycle **10:**2064–2068.
26. **Mossman K.** 2005. Analysis of anti-interferon properties of the herpes simplex virus type I ICP0 protein. Methods Mol. Med. **116:**195–205.
27. **Paladino P, Collins SE, Mossman KL.** 2010. Cellular localization of the herpes simplex virus ICP0 protein dictates its ability to block IRF3-mediated innate immune responses. PLoS One **5:**e10428. doi:10.1371/journal.pone.0010428.
28. **Melroe GT, DeLuca NA, Knipe DM.** 2004. Herpes simplex virus 1 has multiple mechanisms for blocking virus-induced interferon production. J. Virol. **78:**8411–8420.
29. **Lin R, Noyce RS, Collins SE, Everett RD, Mossman KL.** 2004. The herpes simplex virus ICP0 RING finger domain inhibits IRF3- and IRF7-mediated activation of interferon-stimulated genes. J. Virol. **78:**1675–1684.
30. **Mossman KL, Smiley JR.** 2002. Herpes simplex virus ICP0 and ICP34.5 counteract distinct interferon-induced barriers to virus replication. J. Virol. **76:**1995–1998.
31. **Verpooten D, Ma Y, Hou S, Yan Z, He B.** 2009. Control of TANK-binding kinase 1-mediated signaling by the $\gamma_1$34.5 protein of herpes simplex virus 1. J. Biol. Chem. **284:**1097–1105.
32. **Yao XD, Rosenthal KL.** 2011. Herpes simplex virus type 2 virion host shutoff protein suppresses innate dsRNA antiviral pathways in human vaginal epithelial cells. J. Gen. Virol. **92:**1981–1993.
33. **Elgadi MM, Hayes CE, Smiley JR.** 1999. The herpes simplex virus vhs protein induces endoribonucleolytic cleavage of target RNAs in cell extracts. J. Virol. **73:**7153–7164.
34. **Johnson KE, Song B, Knipe DM.** 2008. Role for herpes simplex virus 1 ICP27 in the inhibition of type I interferon signaling. Virology **374:**487–494.
35. **Johnson KE, Knipe DM.** 2010. Herpes simplex virus-1 infection causes the secretion of a type I interferon-antagonizing protein and inhibits signaling at or before Jak-1 activation. Virology **396:**21–29.
36. **Xing J, Wang S, Lin R, Mossman KL, Zheng C.** 2012. Herpes simplex virus 1 tegument protein US11 downmodulates the RLR signaling pathway via direct interaction with RIG-I and MDA-5. J. Virol. **86:**3528–3540.
37. **Xing J, Ni L, Wang S, Wang K, Lin R, Zheng C.** 2013. Herpes simplex virus 1-encoded tegument protein VP16 abrogates the production of beta interferon (IFN) by inhibiting NF-κB activation and blocking IFN regulatory factor 3 to recruit its coactivator CBP. J. Virol. **87:**9788–9801.
38. **Wang S, Wang K, Li J, Zheng C.** 2013. Herpes simplex virus 1 ubiquitin-specific protease UL36 inhibits beta interferon production by deubiquitinating TRAF3. J. Virol. **87:**11851–11860.
39. **Piroozmand A, Koyama AH, Shimada Y, Fujita M, Arakawa T, Adachi A.** 2004. Role of Us3 gene of herpes simplex virus type 1 for resistance to interferon. Int. J. Mol. Med. **14:**641–645.
40. **Liang L, Roizman B.** 2008. Expression of gamma interferon-dependent genes is blocked independently by virion host shutoff RNase and by US3 protein kinase. J. Virol. **82:**4688–4696.
41. **Peri P, Mattila RK, Kantola H, Broberg E, Karttunen HS, Waris M, Vuorinen T, Hukkanen V.** 2008. Herpes simplex virus type 1 Us3 gene deletion influences toll-like receptor responses in cultured monocytic cells. Virol. J. **5:**140.
42. **Chuluunbaatar U, Roller R, Mohr I.** 2012. Suppression of extracellular signal-regulated kinase activity in herpes simplex virus 1-infected cells by the Us3 protein kinase. J. Virol. **86:**7771–7776.
43. **Xing J, Wang S, Lin F, Pan W, Hu CD, Zheng C.** 2011. Comprehensive characterization of interaction complexes of herpes simplex virus type 1 ICP22, UL3, UL4, and UL20.5. J. Virol. **85:**1881–1886.
44. **Zhu H, Zheng C, Xing J, Wang S, Li S, Lin R, Mossman KL.** 2011. Varicella-zoster virus immediate-early protein ORF61 abrogates the IRF3-mediated innate immune response through degradation of activated IRF3. J. Virol. **85:**11079–11089.
45. **Xing J, Wang S, Li Y, Guo H, Zhao L, Pan W, Lin F, Zhu H, Wang L, Li M, Zheng C.** 2011. Characterization of the subcellular localization of herpes simplex virus type 1 proteins in living cells. Med. Microbiol. Immunol. **200:**61–68.
46. **Ehrhardt C, Kardinal C, Wurzer WJ, Wolff T, von Eichel-Streiber C, Pleschka S, Planz O, Ludwig S.** 2004. Rac1 and PAK1 are upstream of IKK-epsilon and TBK-1 in the viral activation of interferon regulatory factor-3. FEBS Lett. **567:**230–238.
47. **Paz S, Vilasco M, Arguello M, Sun Q, Lacoste J, Nguyen TL, Zhao T, Shestakova EA, Zaari S, Bibeau-Poirier A, Servant MJ, Lin R, Meurs EF, Hiscott J.** 2009. Ubiquitin-regulated recruitment of IκB kinase ε to the MAVS interferon signaling adapter. Mol. Cell. Biol. **29:**3401–3412.
48. **Zhao T, Yang L, Sun Q, Arguello M, Ballard DW, Hiscott J, Lin R.** 2007. The NEMO adaptor bridges the nuclear factor-kappaB and interferon regulatory factor signaling pathways. Nat. Immunol. **8:**592–600.
49. **Yoneyama M, Kikuchi M, Natsukawa T, Shinobu N, Imaizumi T, Miyagishi M, Taira K, Akira S, Fujita T.** 2004. The RNA helicase RIG-I has an essential function in double-stranded RNA-induced innate antiviral responses. Nat. Immunol. **5:**730–737.
50. **Chang TH, Liao CL, Lin YL.** 2006. Flavivirus induces interferon-beta gene expression through a pathway involving RIG-I-dependent IRF-3 and PI3K-dependent NF-kappaB activation. Microbes Infect. **8:**157–171.
51. **Kochs G, Garcia-Sastre A, Martinez-Sobrido L.** 2007. Multiple anti-interferon actions of the influenza A virus NS1 protein. J. Virol. **81:**7011–7021.
52. **Lin R, Lacoste J, Nakhaei P, Sun Q, Yang L, Paz S, Wilkinson P, Julkunen I, Vitour D, Meurs E, Hiscott J.** 2006. Dissociation of a MAVS/IPS-1/VISA/Cardif-IKKε molecular complex from the mitochondrial outer membrane by hepatitis C virus NS3-4A proteolytic cleavage. J. Virol. **80:**6072–6083.
53. **Wang S, Liu N, Chen AJ, Zhao XF, Wang JX.** 2009. TRBP homolog interacts with eukaryotic initiation factor 6 (eIF6) in Fenneropenaeus chinensis. J. Immunol. **182:**5250–5258.
54. **Wang S, Shi LJ, Liu N, Chen AJ, Zhao XF, Wang JX.** 2012. Involvement of *Fenneropenaeus chinensis* cathepsin C in antiviral immunity. Fish Shellfish Immunol. **33:**821–828.
55. **Jordan M, Schallhorn A, Wurm FM.** 1996. Transfecting mammalian cells: optimization of critical parameters affecting calcium-phosphate precipitate formation. Nucleic Acids Res. **24:**596–601.
56. **Zhong B, Yang Y, Li S, Wang YY, Li Y, Diao F, Lei C, He X, Zhang L, Tien P, Shu HB.** 2008. The adaptor protein MITA links virus-sensing receptors to IRF3 transcription factor activation. Immunity **29:**538–550.
57. **Xing J, Wu F, Pan W, Zheng C.** 2010. Molecular anatomy of subcellular

localization of HSV-1 tegument protein US11 in living cells. Virus Res. **153:**71–81.
58. **Iwamura T, Yoneyama M, Yamaguchi K, Suhara W, Mori W, Shiota K, Okabe Y, Namiki H, Fujita T.** 2001. Induction of IRF-3/-7 kinase and NF-kappaB in response to double-stranded RNA and virus infection: common and unique pathways. Genes Cells **6:**375–388.
59. **Kawaguchi Y, Kato K, Tanaka M, Kanamori M, Nishiyama Y, Yamanashi Y.** 2003. Conserved protein kinases encoded by herpesviruses and cellular protein kinase cdc2 target the same phosphorylation site in eukaryotic elongation factor 1δ. J. Virol. **77:**2359–2368.
60. **Li Y, Wang S, Zhu H, Zheng C.** 2011. Cloning of the herpes simplex virus type 1 genome as a novel luciferase-tagged infectious bacterial artificial chromosome. Arch. Virol. **156:**2267–2272.
61. **Li Y, Zhao L, Wang S, Xing J, Zheng C.** 2012. Identification of a novel NLS of herpes simplex virus type 1 (HSV-1) VP19C and its nuclear localization is required for efficient production of HSV-1. J. Gen. Virol. **93:**1869–1875.
62. **Tischer BK, von Einem J, Kaufer B, Osterrieder N.** 2006. Two-step red-mediated recombination for versatile high-efficiency markerless DNA manipulation in Escherichia coli. Biotechniques **40:**191–197.
63. **Alexopoulou L, Holt AC, Medzhitov R, Flavell RA.** 2001. Recognition of double-stranded RNA and activation of NF-kappaB by Toll-like receptor 3. Nature **413:**732–738.
64. **Takahasi K, Yoneyama M, Nishihori T, Hirai R, Kumeta H, Narita R, Gale M, Jr, Inagaki F, Fujita T.** 2008. Nonself RNA-sensing mechanism of RIG-I helicase and activation of antiviral immune responses. Mol. Cell **29:**428–440.
65. **Deruelle MJ, Favoreel HW.** 2011. Keep it in the subfamily: the conserved alphaherpesvirus US3 protein kinase. J. Gen. Virol. **92:**18–30.
66. **Vandevenne P, Lebrun M, El Mjiyad N, Ote I, Di Valentin E, Habraken Y, Dortu E, Piette J, Sadzot-Delvaux C.** 2011. The varicella-zoster virus ORF47 kinase interferes with host innate immune response by inhibiting the activation of IRF3. PLoS One **6:**e16870. doi:10.1371/journal.pone.0016870.
67. **Devaraj SG, Wang N, Chen Z, Tseng M, Barretto N, Lin R, Peters CJ, Tseng CT, Baker SC, Li K.** 2007. Regulation of IRF-3-dependent innate immunity by the papain-like protease domain of the severe acute respiratory syndrome coronavirus. J. Biol. Chem. **282:**32208–32221.
68. **Zhang Z, Zheng Z, Luo H, Meng J, Li H, Li Q, Zhang X, Ke X, Bai B, Mao P, Hu Q, Wang H.** 2012. Human bocavirus NP1 inhibits IFN-beta production by blocking association of IFN regulatory factor 3 with IFNB promoter. J. Immunol. **189:**1144–1153.
69. **Melroe GT, Silva L, Schaffer PA, Knipe DM.** 2007. Recruitment of activated IRF-3 and CBP/p300 to herpes simplex virus ICP0 nuclear foci: potential role in blocking IFN-beta induction. Virology **360:**305–321.
70. **Purves FC, Deana AD, Marchiori F, Leader DP, Pinna LA.** 1986. The substrate specificity of the protein kinase induced in cells infected with herpesviruses: studies with synthetic substrates [corrected] indicate structural requirements distinct from other protein kinases. Biochim. Biophys. Acta **889:**208–215.
71. **Benetti L, Roizman B.** 2004. Herpes simplex virus protein kinase US3 activates and functionally overlaps protein kinase A to block apoptosis. Proc. Natl. Acad. Sci. U. S. A. **101:**9411–9416.
72. **Daikoku T, Yamashita Y, Tsurumi T, Maeno K, Nishiyama Y.** 1993. Purification and biochemical characterization of the protein kinase encoded by the US3 gene of herpes simplex virus type 2. Virology **197:**685–694.
73. **Eisfeld AJ, Turse SE, Jackson SA, Lerner EC, Kinchington PR.** 2006. Phosphorylation of the varicella-zoster virus (VZV) major transcriptional regulatory protein IE62 by the VZV open reading frame 66 protein kinase. J. Virol. **80:**1710–1723.
74. **Kumar KP, McBride KM, Weaver BK, Dingwall C, Reich NC.** 2000. Regulated nuclear-cytoplasmic localization of interferon regulatory factor 3, a subunit of double-stranded RNA-activated factor 1. Mol. Cell. Biol. **20:**4159–4168.
75. **Wang JT, Doong SL, Teng SC, Lee CP, Tsai CH, Chen MR.** 2009. Epstein-Barr virus BGLF4 kinase suppresses the interferon regulatory factor 3 signaling pathway. J. Virol. **83:**1856–1869.